Electronic Supplementary Material (ESI) for Journal of Materials Chemistry C.

Supporting Information

Quantitative Understanding of the Ultra-Sensitive and Selective Detection of Dopamine using Graphene Oxide/WS_2 Quantum Dot Hybrid

Ruma Das[a], Abhilasha Bora[a], and P. K. Giri[a, b*]

[a]*Department of Physics, Indian Institute of Technology Guwahati, Guwahati -781039, India.*

[b]*Centre for Nanotechnology, Indian Institute of Technology Guwahati, Guwahati -781039, India.*

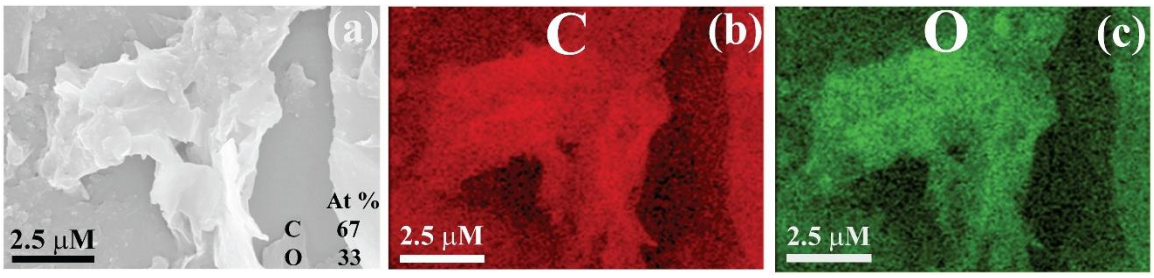

Fig. S1: (a) FESEM image of GO with atomic % of elemental compositions in the inset. (b, c) Elemental mapping on the same GO sheets for C and O elements, respectively.

* Corresponding author, email: giri@iitg.ac.in

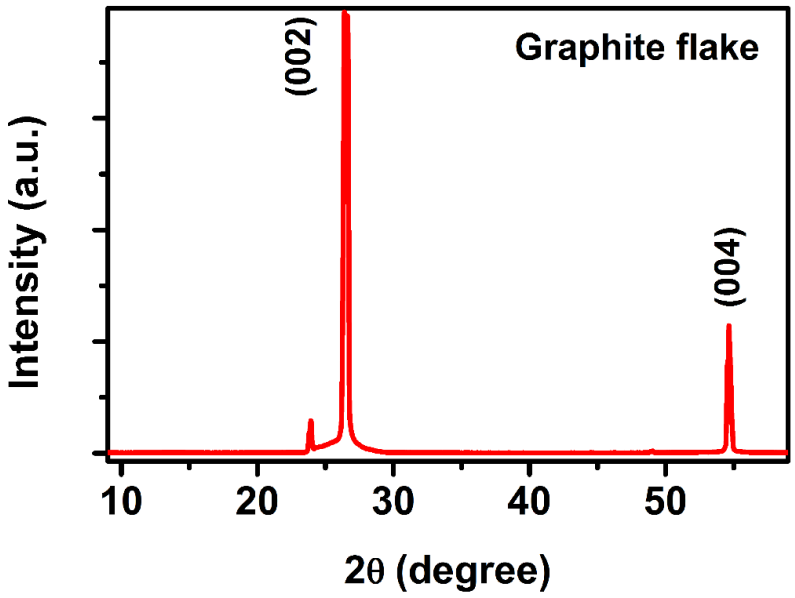

Fig. S2: XRD pattern of pristine graphite flakes.

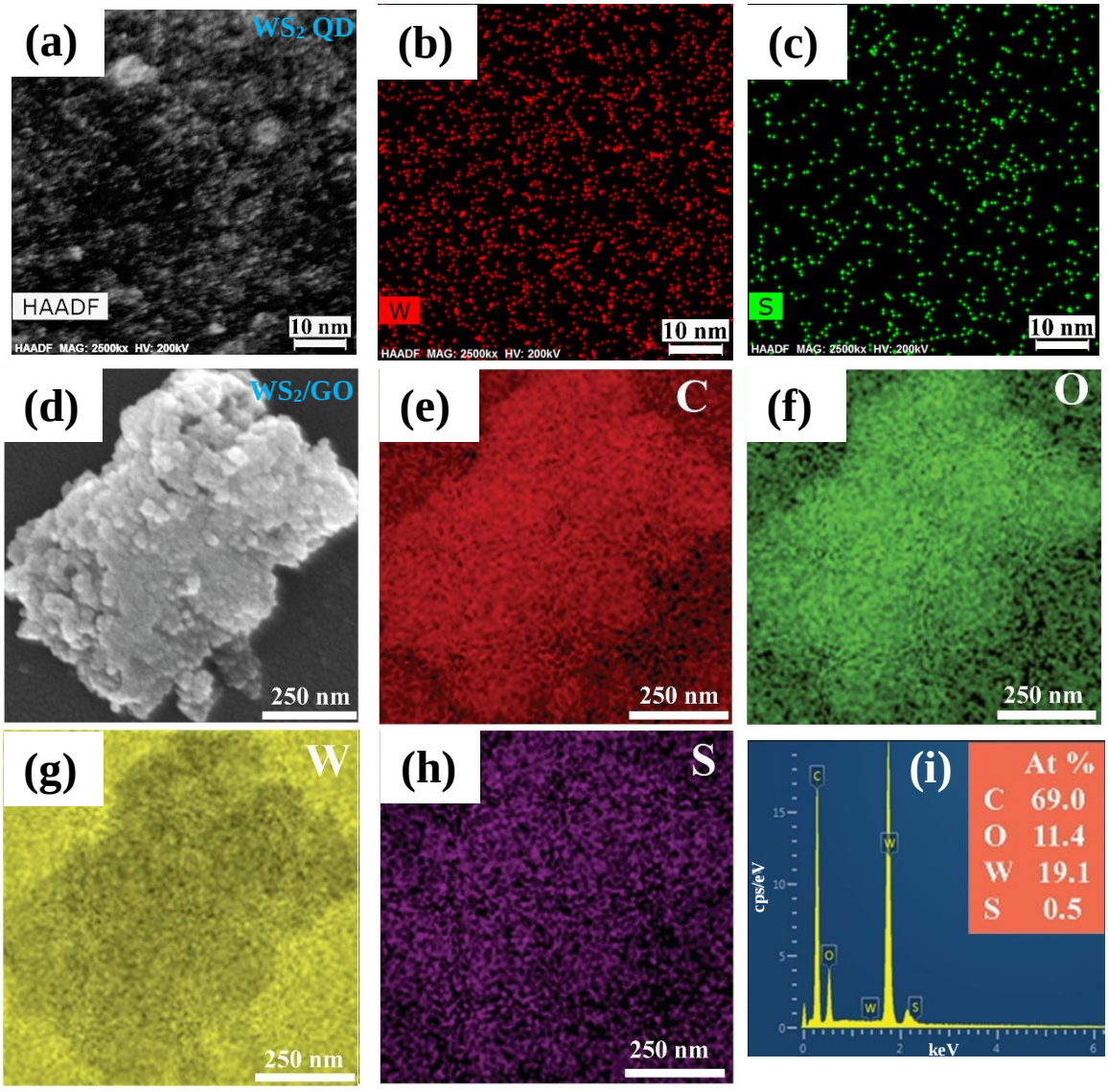

Fig. S3: (a) HAADF image of WS_2 QDs and (b, c) the corresponding elemental mapping of the sample showing the spatial distribution of W and S, respectively. (d) FESEM image of WS_2/GO hybrid. (e-h) Elemental mapping on (d) for C, O, W, and S, respectively, and (i) the corresponding EDX spectra with atomic % of elemental compositions.

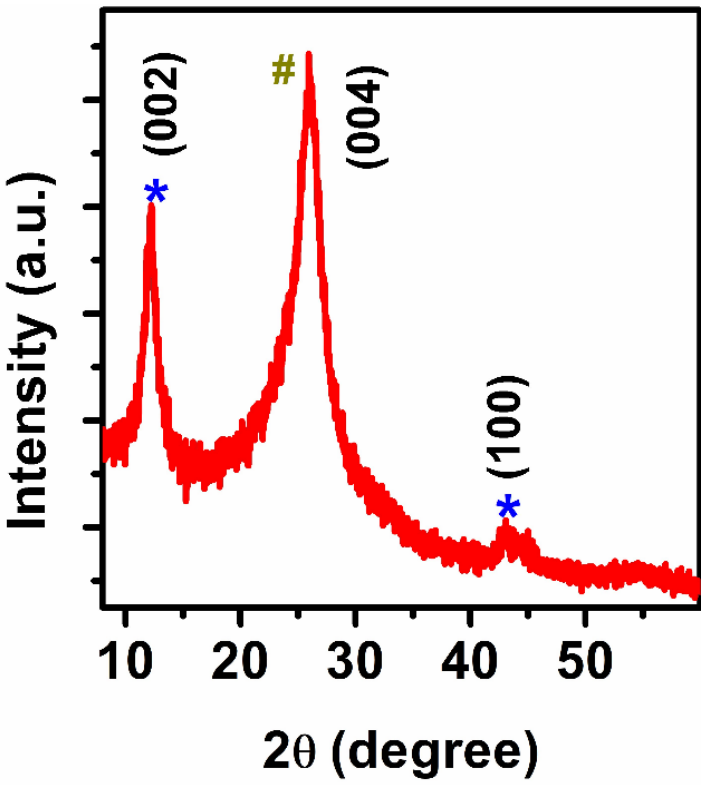

Fig. S4: XRD pattern of WS_2/GO hybrid. The peak position of GO and WS_2 are symbolized by '*' and '#', respectively.

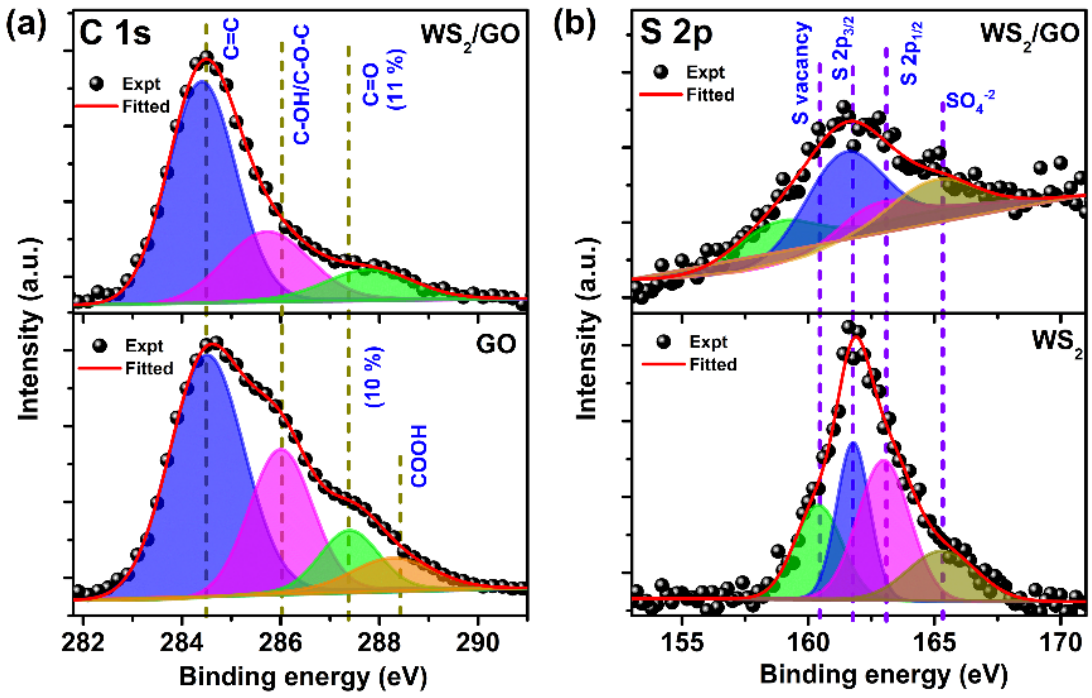

Fig. S5: XPS spectra of (a) C 1s of GO and (b) S 2p of WS_2 before and after WS_2/GO hybrid formation.

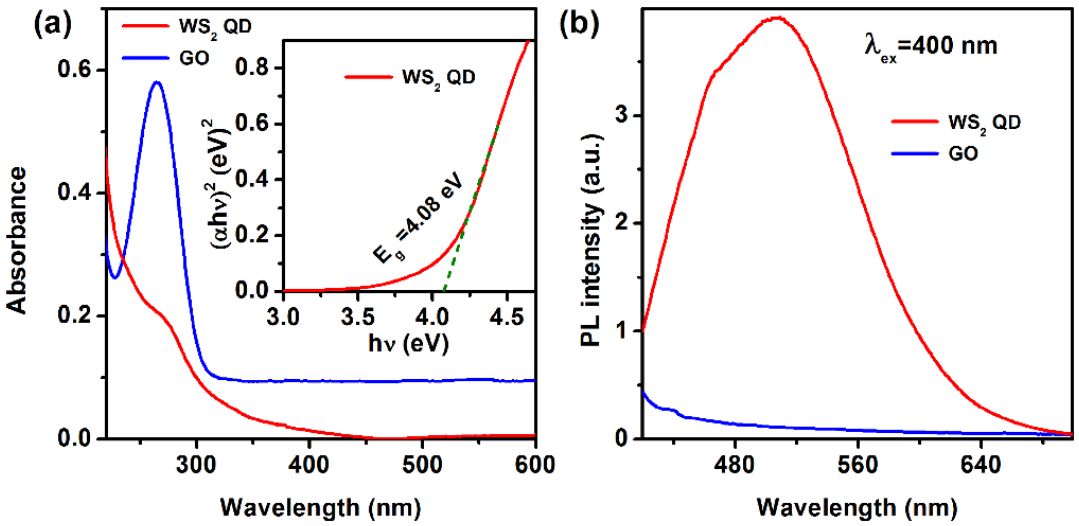

Fig. S6: (a) Absorption spectra of WS_2 QDs and GO sheets. The inset shows the Tauc plot for WS_2 QDs considering its direct band gap. (b) Comparison of the PL spectra of bare WS_2 QDs and GO sheets under 400 nm excitation.

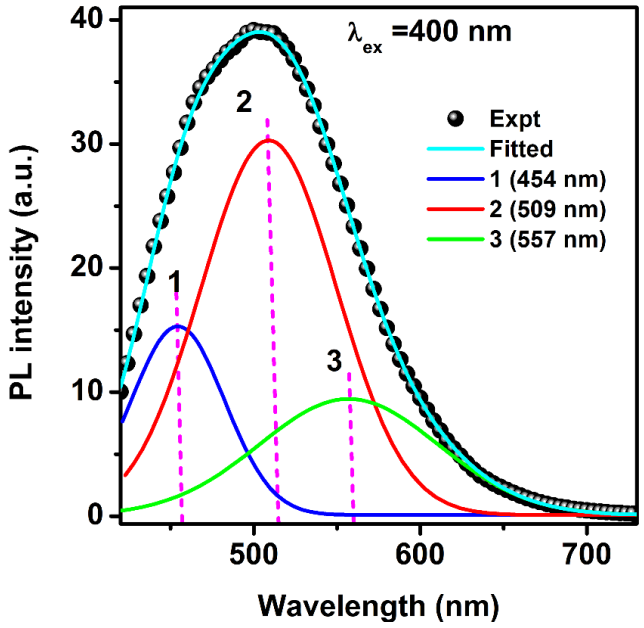

Fig. S7: The Gaussian deconvolution of PL spectrum of WS_2 QDs at λ_{ex} =400 nm.

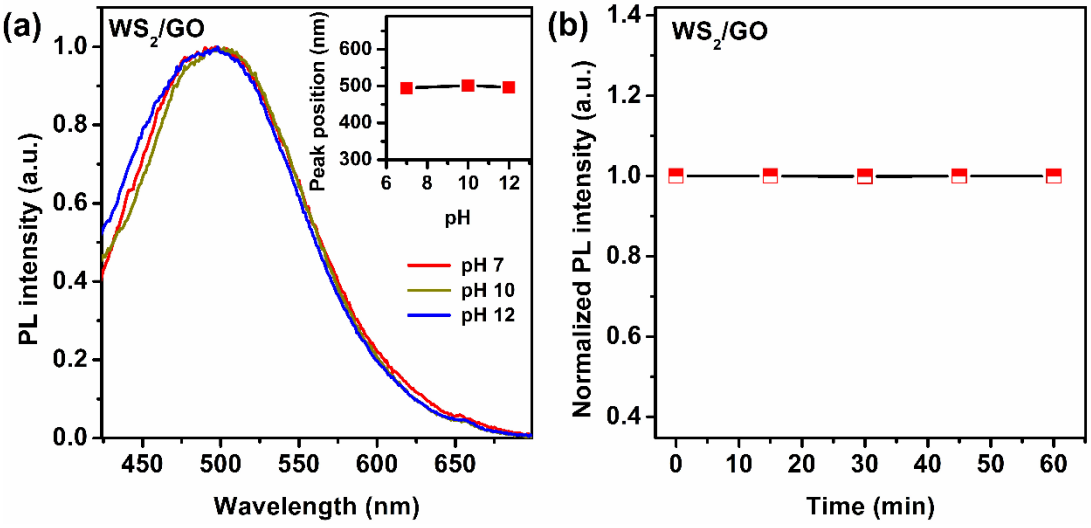

Fig. S8: (a) Normalized PL spectra of WS_2/GO hybrid at different pH. The inset shows the variation of the maximum peak position with pH. (b) Stability of the WS_2/GO hybrid with time.

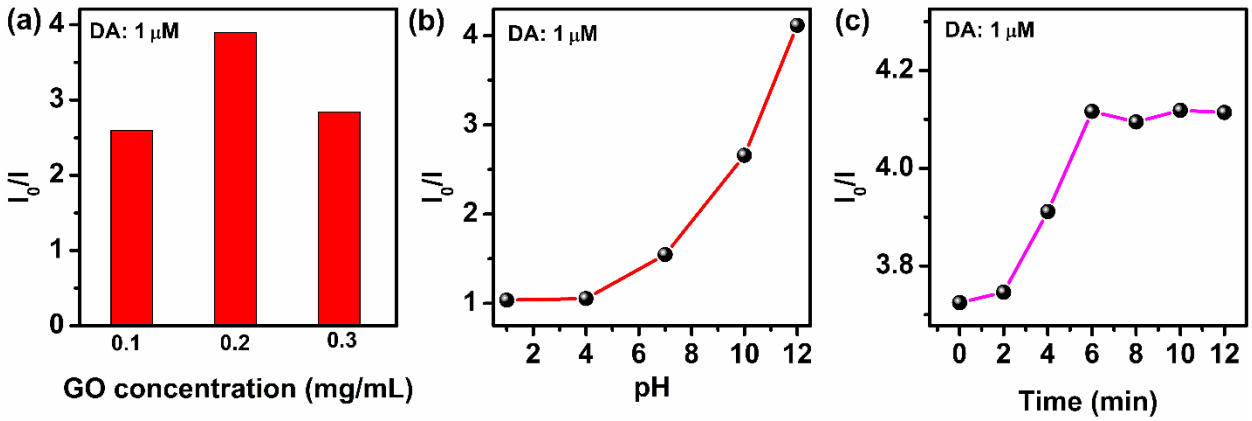

Fig. S9: Optimization of DA sensing: (a) GO concentration, (b) pH value and (c) reaction time with fixed concentration of WS_2 QDs and DA.

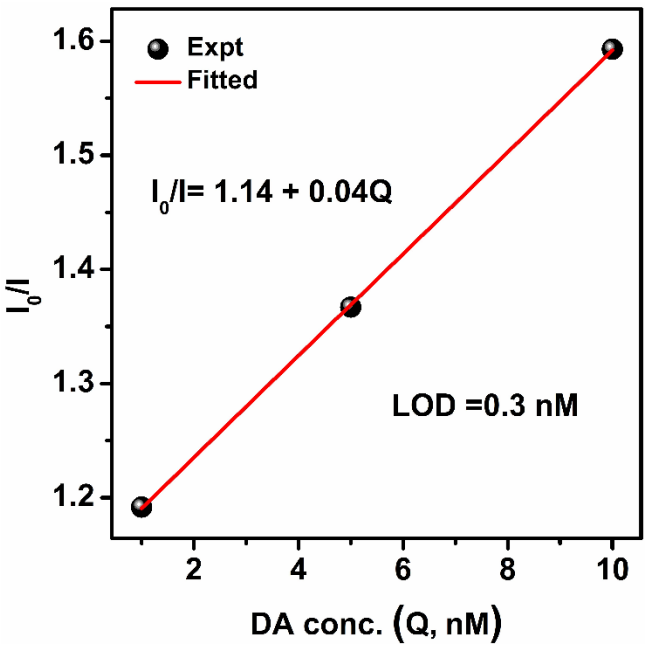

Fig. S10: The linear variation of I_0/I with DA concentration 1–10 nM with LOD 30 nM limit of detection (LOD).

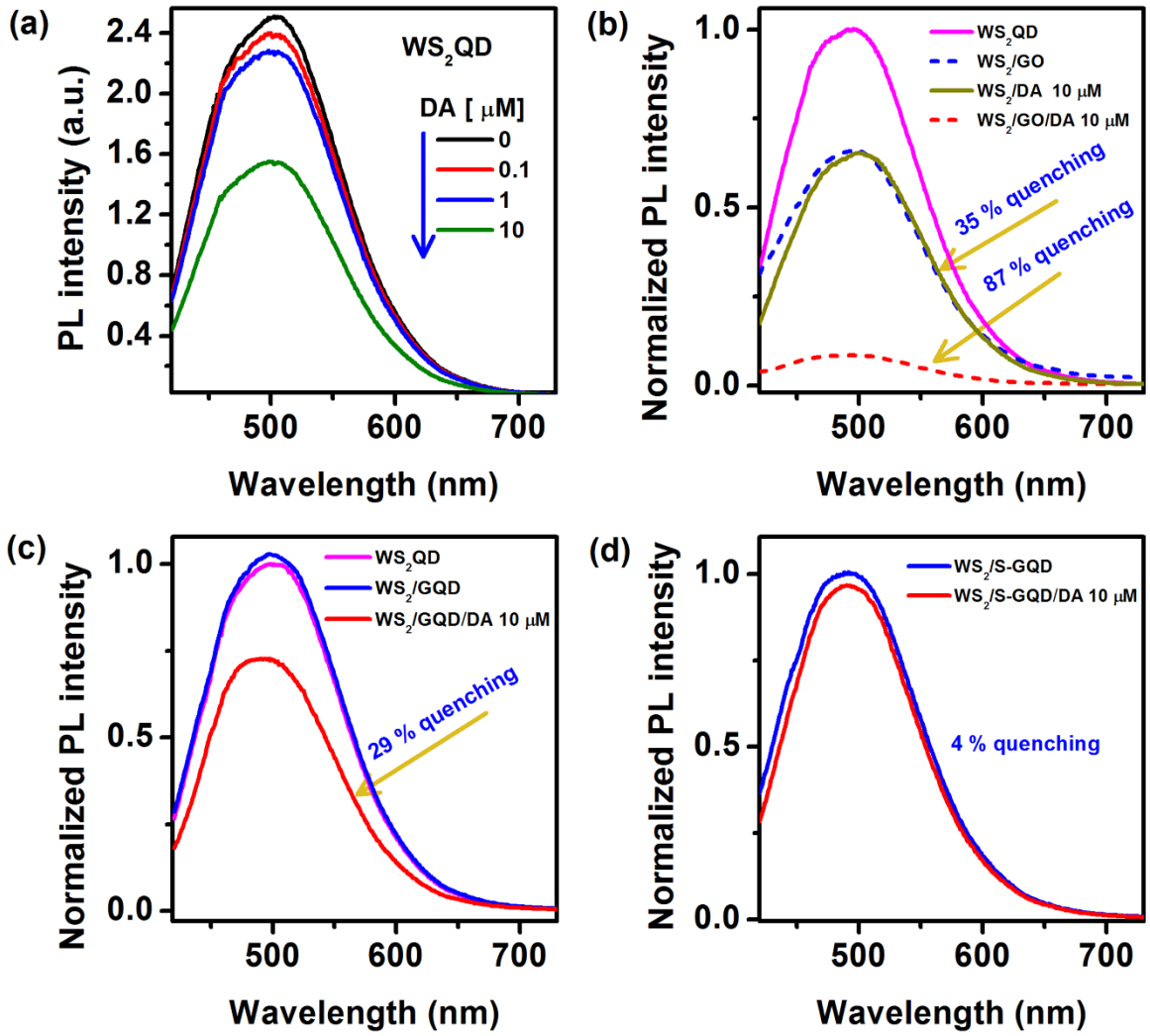

Fig. S11: (a) The change of the PL intensity of WS_2 QDs with the presence of different concentration of DA. Comparison of PL quenching efficiency of (b) GO, (c) GQDs and (d) S-GQDs with fixed concentration of WS_2 QDs and 10 μM DA.

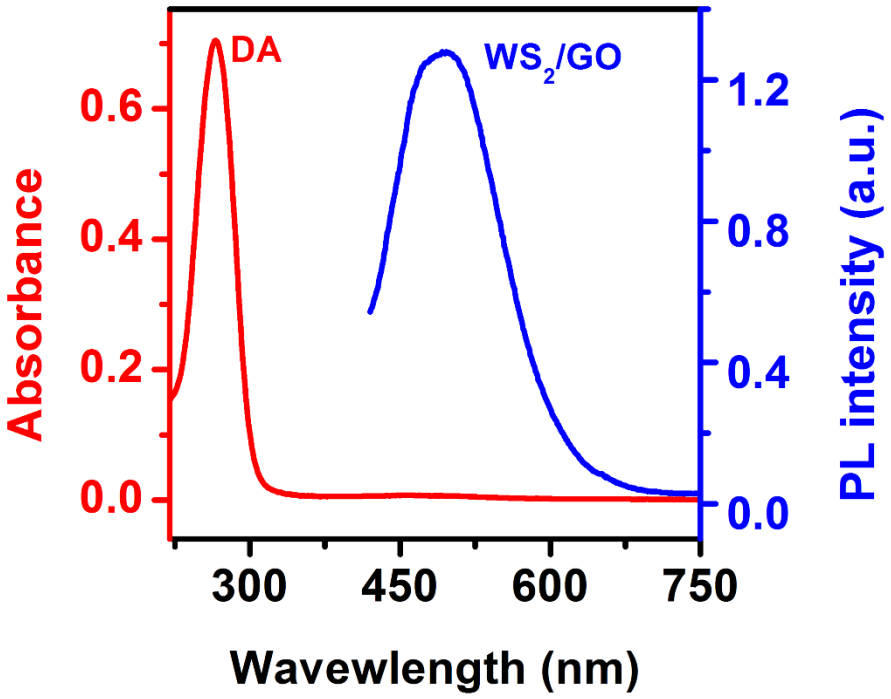

Fig. S12: A large separation between the absorption of DA and the PL of WS_2/GO discards the possibility of FRET process between them.

Table S1: Details of the deconvoluted high resolution XPS spectra of O 1s for GO, WS_2/GO and WS_2/GO/DA.

Sample	Peak position (eV)	Peak identity	% of contribution
GO	530.6	COOH	12
	532.2	C=O	55
	533.4	C-OH/C-O-C	33
WS_2/GO	530.5	COOH	12
	532.0	C=O	66
	533.0	C-OH/C-O-C	22
WS_2/GO/DA	530.4	COOH	8
	531.8	C=O	81
	532.9	C-OH/C-O-C	11

Table S2: Details of the Raman modes of different samples.

Sample	Raman bands (cm^{-1})					
	D	M	G	D'	E_{2g}	A_{1g}
GO	1356	1528	1586	1612	-	-
WS_2 QD	-	-	-	-	357.3	421.4
WS_2/GO	1356	1529	1577	1610	357.3	421.6
WS_2/GO/DA	1356	1531	1582	1611	357.3	422.0
Peak identity	*Defects (GO)*	*Metallic (GO)*	*In-plane vibration of C=C bond (GO)*	*Structural disorder /edges (GO)*	*In-plane vibration of W-S bond (WS_2)*	*Out-of-plane vibration of W-S bond (WS_2)*

Table S3: Summary of the fitting parameters of time resolved PL decay data of WS_2, GO and their hybrid in absence and in presence of DA.

Sample Code	τ_1 (ns)	τ_2 (ns)	B_1 %	B_2 %	τ_{avg} (ns)
WS_2 QD	2.1	9.6	34	66	8.8
WS_2 /GO	1.7	8.8	34	66	8.2
WS_2 /DA	2.3	9.7	39	61	8.8
WS_2 /GO/DA	1.5	4.7	15	85	4.6

Table S4: Detection of DA spiked in Brahmaputra river water and blood serum samples.

Sample	Added concentration of DA (nM)	Found concentration of DA (nM)	Recovery (%)
Brahmaputra river water	1	1 ± 0.007	100
	10	15 ± 0.09	150
	100	81 ± 0.60	81
	1000	720 ± 2.0	72
Blood serum	1	1 ± 0.001	100
	10	10 ± 0.010	100
	100	80 ± 0.2	80
	1000	760 ± 4.0	76